Development 119, 447-456 (1993)
Printed in Great Britain © The Company of Biologists Limited 1993

The zebrafish midblastula transition

Donald A. Kane* and Charles B. Kimmel†

Institute of Neuroscience, University of Oregon, Eugene, Oregon 97403, USA

*Present address: Max Planck Institut für Entwicklungsbiologie, Abteilung III, Spemannstrasse 35, 72076 Tübingen, Germany
†Author for correspondence

SUMMARY

The zebrafish midblastula transition (MBT) begins at cycle 10. It is characterized by cell cycle lengthening, loss of cell synchrony, activation of transcription and appearance of cell motility. Superceding a 15 minute oscillator that controls the first nine cycles, the nucleocytoplasmic ratio appears to govern the MBT. This timing mechanism operates cell autonomously: clones of labeled cells initiate cell cycle lengthening independently of neighbors but dependent on immediate lineal ancestors. Unequal divisions, when they occur, produce asymmetric cell cycle lengthening based on the volume of each daughter. During the several cycles after the MBT begins, cycle length is correlated with the reciprocal of the blastomere volume, suggesting a continuation of cell cycle regulation by the nucleocytoplasmic ratio during an interval that we term the 'MBT period'.

Key words: cleavage, blastula, transcriptional activation, time-lapse microscopy, cell cycle, nucleocytoplasmic ratio, cell motility, cytoplasmic volume

INTRODUCTION

The early development of many animals is characterized by rapid and synchronous cleavages that quickly subdivide the zygote into a large population of blastomeres. This stage is followed by a midblastula transition (MBT) to a longer cell cycle that is accompanied by the loss of cell synchrony (Signoret and Lefresne, 1971; Gerhart, 1980), and activation of transcription and cell motility (Newport and Kirschner, 1982a), both characteristics essential for the ensuing process of gastrulation.

The lengthening of the cell cycle is thought to be the primary cause of many of the associated behaviors at MBT. If inhibitors are used to stop the cell cycle early in *Drosophila*, then transcriptional activation occurs early (Edgar and Schubiger, 1986) and, in *Xenopus*, both onset of cell motility and activation of transcription occur early (Kimelman et al., 1987).

MBT begins when the cleaving cells reach a particular nucleocytoplasmic ratio: MBT is late in haploid embryos (Signoret and Lefresne, 1973; Edgar and Schubiger, 1986) and is early in tetraploid or polyploid embryos (Newport and Kirschner, 1982a; Mita and Obata, 1984). MBT also occurs early when the nucleocytoplasmic ratio is increased by ligating a portion of the cytoplasm away from the early nuclei in the early fly blastula (Edgar and Schubiger, 1986), in starfish embryos (Mita and Obata, 1984) and in the newt (Kobayakawa and Kubota, 1981). Ligating frog embryos (Newport and Kirschner, 1982a), similar to the classic experiment by Spemann on *Triturus* (Spemann, 1938), suggest that neither absolute time nor counting models of MBT timing are likely MBT-triggering mechanisms.

The basis for the loss of synchrony at MBT is not understood. One idea, which we propose and examine here, is that individual cells or lineages of cells could start their MBT cell cycle lengthening based on their individual volumes, which would give each of them a unique nucleocytoplasmic ratio. The volume differences of individual cells could be — by chance or design — the result of unequal earlier cleavage divisions. This hypothesis is consistent with the mitotic behavior of invertebrate embryos which have early, extremely unequal cleavages, such as in sea urchin micromere formation (Okazaki, 1975), in *Caenorhabditis* P-blast lineage divisions (Sulston et al., 1983) and in leech teloblast divisions (Bissen and Weisblat, 1989). An alternative view, though not mutually exclusive, is that as cells become specified to different programs of development, these differences are subsequently mirrored in differential lengthening of the cell cycle. Evidence for this hypothesis comes from the study of mitotic domains in the fly embryo, where during cycle 14 the cell cycle of patches of cells correlates to cell fate (Foe, 1989) and mutations that change cell fate change cell cycle length (Arora and Nüsslein-Volhard, 1992).

MBT in teleosts is not well characterized. During cleavage cycles 1 to 7, divisions are stereotyped and highly synchronous (Oppenheimer, 1936, 1937; Hisaoka and Battle, 1958), each consecutive cycle having approximately the same length (Roosen-Runge, 1938; Marrable, 1959). At the blastula stage, beginning at cycle 8, the embryos show slight metasynchrony, with waves of mitosis emanating

from the animal pole; during this time, Marrable (1965) reported a gradual increase in the cell cycle in the zebrafish, indicating possible MBT-like cell cycle lengthening. In studies on the loach, *Misgurnus fossilis*, Rott and Shevelava (1967) found a more defined cell cycle lengthening, which did not occur until cycle 11, and, in the same study, they found the equivalent cell cycle lengthening in haploid embryos occurred at cycle 12, indicating that onset of teleost cell cycle lengthening is timed by the nucleocytoplasmic ratio. Motility of cells in the early blastula stage has not been reported, but cells are motile by the late blastula stage, as established for *Fundulus* (Trinkaus and Erickson, 1983) and zebrafish (Thomas and Waterman, 1978). Therefore, although studies of teleosts are incomplete, many of the elements of a frog-like MBT seem to be present.

In this paper, as a prelude to studies relating the blastula cell cycle to cell fate, we characterize the zebrafish MBT and examine the role that the nucleocytoplasmic ratio plays in cell cycle control during the MBT. We find that cell cycle lengthening and loss of cell synchrony begins at cycle 10, with a concomitant activation of transcription and motility. The timing of MBT onset appears to be under the control of the nucleocytoplasmic ratio. Afterwards, during the next several cycles, we find a correlation of the cell volume — and hence nucleocytoplasmic ratio — with cycle lengths, suggesting that the rapid loss of cell synchrony at MBT is based on unequal cell division. Finally, we examine a potential role for the nucleocytoplasmic ratio in cell cycle control during early development.

MATERIALS AND METHODS

Embryos

Eggs were produced for experiments by either natural crosses or by in vitro fertilization (Streisinger et al., 1981). All embryos with experimental ploidys were fertilized in vitro with the following modifications: activated eggs were produced by activation with the addition of water without the addition of sperm and are equivalent to unfertilized eggs. Haploid embryos were produced by fertilization with sperm inactivated by a short exposure to ultraviolet irradiation. Tetraploid eggs were produced by fertilization with untreated sperm but then briefly exposed to heat to prevent the first mitotic division, a method used for the production of clonal diploids.

Dye injections

After fertilization, embryos were maintained at 28.5±1°C in E medium (13.7 mM NaCl, 0.5 mM KCl, 1.3 mM $CaCl_2$, 1 mM $MgSO_4$, 4.2 mM $NaHCO_3$ and 0.07 mM sodium/potassium phosphate buffer, pH 7.2). From early cleavage until dye injections, embryos were time-lapse recorded at low power to confirm their developmental stage. Cells were injected as described (Kimmel et al., 1990) using 50 mg/ml tetramethylrhodamine-isothiocyanate dextran (10,000 M_r; Molecular Probes, Eugene, Oregon) in 0.2 M KCl as the lineage tracer.

Microscopy

Observations were made on a Zeiss Universal microscope equipped with Nomarski differential interference contrast optics and UV epilumination. In later experiments, the microscopes were also equipped with a motor driven focus controller and motor driven shutters for the white light and UV sources, all computer controlled (Applied Scientific Instrumentation, Eugene, Oregon). The microscope objectives used for time-lapse recordings were either a Zeiss 40× water immersion (N.A.= 0.7) or Leitz 50× water immersion (N.A.= 1.0) using the Nomarski upper prism for a Zeiss 63× variable immersion lens. Embryos were immobilized with 0.1% agarose in E medium. Viewing chambers were constructed of two 60×22 mm no. 1 coverslips separated with three pairs of 18×18 mm no. 1 coverglass spacers; the chamber edges were sealed with Vaseline to prevent evaporation.

Time-lapse recordings

A high resolution camera (GE, model series 68) was used to record single frame images to a video recorder (Gyre) similar to that described (Warga and Kimmel, 1990; Kane and Warga, 1991). For later experiments, single frame images were recorded on an Optical Memory Disc Recorder (Panasonic, model no. 3040) using a computer to control the plane of focus, UV and white light shutters (Kane et al., 1992). For recordings of cells containing lineage tracing dyes, we used low levels of UV illumination to prevent damage to the dye-filled cells and a Silicon Intensified Target video camera (Dage) to record frames. Low-light images were computer enhanced before recording. A Mac II Computer (Apple Computer Corporation) equipped with digitizing board (QuickCapture) and an auxiliary monitor output (RasterOps) running Neurovideo 2.96 software (Myers and Bastiani, 1991) was used for time-lapse control, image enhancement and generating playback sequences.

Cell cycle measurements

The breakdown of the nuclear membrane was used as the event marker for the end of one cell cycle and the beginning of the next.

For the majority of the time-lapse recordings, the shortest and longest cell cycles were deduced for each mitotic cycle. The shortest cell cycle was taken as the time separating the first cells to enter mitosis in the divisions before and after the interphase corresponding to the cycle; the longest cell cycle was taken as the time separating the last cells to enter mitosis in the divisions before and after the same interphase. The range of cycle lengths for each cell cycle is the difference between the two time values.

The validity of the above method was verified by a second method where we carefully measured the cell cycle of each individual cell in the field of exceptionally stable 4-dimensional time-lapse recordings in which a >90% of the cells could be traced throughout the length of their cell cycle.

Motility measurements

The presence of motile cells was determined from the presence of pseudopods and the erratic side-to-side movement of cells apparent in time-lapse recordings. For recordings of individual cells, identified cells were selected from descendants of dye-injected cells that were time-lapse recorded in multiple focal planes. Images were traced from the video monitor.

RNA measurements

A mixture of 5 parts ^{32}P-labeled UTP (600 Ci/mmole) and 1 part 10% phenol red was drawn into a rotary driven pipette by suction and injected into the yolk during the 4- and 8-cell stages, when all of the cells in the embryo are cytoplasmically continuous with the yolk. The injection volume was 1 nl ± 50%.

At various time points, embryos, carried in 20 μl of E medium, were added to 20 μl 10% sodium dodecyl sulfate, dissolved and added to 155 μl of a solution of 25 mM EDTA, 12.5 mM Tris (pH 7.0) and 125 μg/ml tRNA. Proteinase K was added at a concentration of 250 μg/ml and the sample was incubated 1 hour at 50°C. An aliquot was scintillation counted to measure the initial injection volume and the remainder of the sample was extracted once with two volumes of phenol:chloroform:iso-amyl alcohol (24:24:1), and

once with one volume of chloroform:iso-amyl alcohol (24:1). Sodium acetate was added to a final concentration of 1%, the sample was ethanol precipitated (1 hour at −70°C) and nucleic acids were resuspended in water.

Controls were as above except tRNA carrier was replaced with 100 μg/ml calf thymus DNA and samples were incubated with 100 μg/ml RNAseA at 37°C for 1 hour.

For scintillation counting, the entire sample volume was added to 10 μl 100% TCA on a Whatman GF-F filter, the filter was rinsed with 10 ml 7% TCA, followed by 100% ethanol, dried and counted in 5 ml EcoScint.

RNA was electrophoresed on 1.2% agarose with 7% formamide according to Maniatis et al. (1982), dried on a Hoefer gel dryer and exposed to Kodak XAR-5 film at −70°C.

Enucleation experiments

The apparatus for removal of nuclei consisted of a 10 μl Hamilton syringe mounted in a rotary drive as described (Ho and Kane, 1990), except that the tip of the pipette was broken off to a diameter of 20 μm and not fire polished.

At 30 to 35 minutes postfertilization, when the first cleavage furrow can first be seen, embryos were mounted in a gel of 3% methylcellulose in E medium, and nuclei were aspirated with part of the cell membrane into the pipette.

Cell volume measurements

During early mitosis, deep cells are spherical and turgid, inferred from the bulging of the cells into surrounding interphase cells. For cell volume observations, we made time-lapse recordings of deep cells at multiple planes of focus and, for each cell, compared several planes of focus during early mitosis to find the most circular outline of the cell and from that estimated the volume of the cell. Enveloping layer cells were excluded from this analysis because they did not completely round up during mitosis.

RESULTS

Cell cycle lengthening and loss of cell synchrony begin at cycle 10

At the MBT cell cycles lengthen and lose synchrony (Newport and Kirschner, 1982a). To establish when these changes occur in zebrafish, we made time-lapse recordings from early cleavage until the beginning of epiboly (about cycle 13), focusing in particular on cycle-related changes in cell nuclei (Fig. 1). The nuclear disappearance in early mitosis, and reappearance some minutes after cytokinesis, provides a precise measure of cycle length, as well as its subdivision into periods of interphase and mitosis.

In several exceptionally stable time-lapse recordings, we could determine cycle length of every cell in the field of view during several cycles (Fig. 2A). During cleavage, and until the ninth zygotic cell cycle, all of the cells in the field divide synchronously with a cycle length of 14 to 15 minutes. We first detect cycle lengthening, of about 10%, at cycle 10. This increase is statistically significant when the results of all embryos are combined (Table 1; $P<0.01$, Wilcoxon Signed Rank Test; $n=19$). The cycle lengthening is statistically significant in our recordings on an embryo

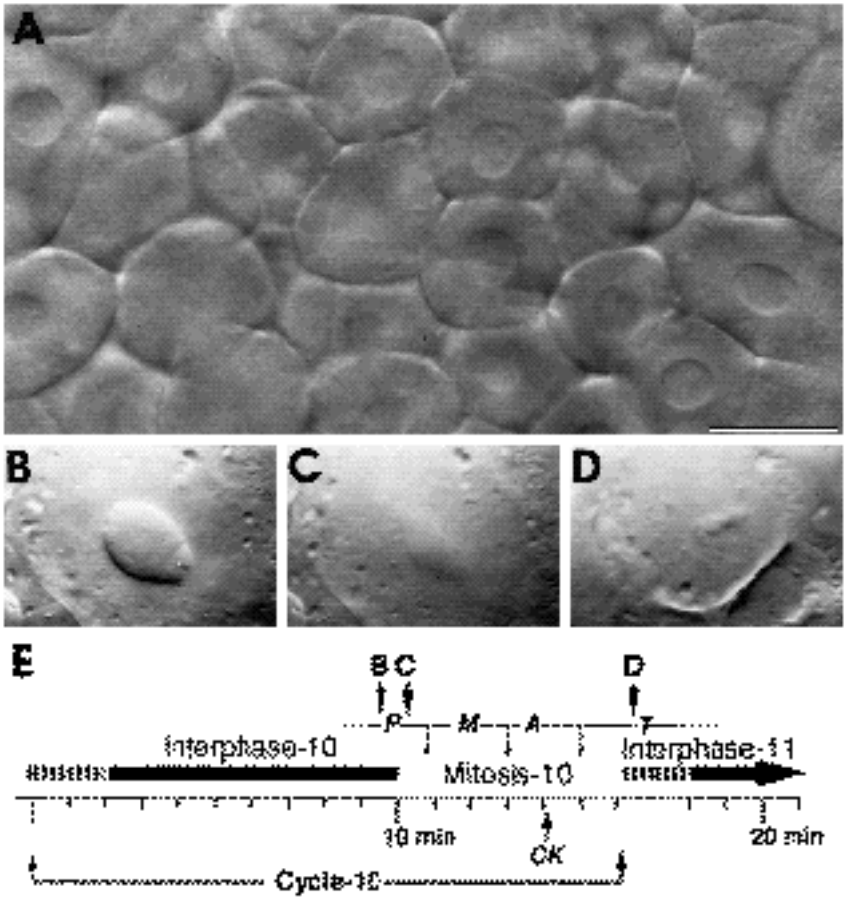

Fig. 1. Sequence of events during the blastula cell cycle. (A-D) Microphotographs showing blastomeres visualized during time-lapse recordings using Nomarski DIC optics. (A) Low-power view of cycle 11 cells, some in interphase, some in early mitosis (of division 11). Cycle 11 corresponds to the 1K-cell stage of Warga and Kimmel (1990) in the midblastula. (B-D) High-power views. (B) Late interphase/early prophase nucleus during cycle 10. (C) Same nucleus, 45 seconds later, in prophase of division 10, just before the nuclear membrane is completely lost. (D) Early telophase, showing the telophase nuclei, which condense as disk-shaped arrays of vesicles with their planar axes parallel to the plane of the newly formed cleavage furrow. Note that the shape of the interphase nucleus predicts the axis of cytokinesis. Scale bar is 25 μm for A and 15 μm for B-D. (E) Sequence of events in the cell cycle of the individual cell shown in B-D. Solid line indicates time in interphase, space indicates time in mitosis and dashed pattern indicates the time when the returning telophase nuclei can be faintly seen. The abscissa indicates minutes relative to the beginning of cycle 10. Roman letters refer to photographs above. Abbreviations: P, prophase; M, metaphase; A, anaphase; T, telophase; CK, beginning of cytokinesis.

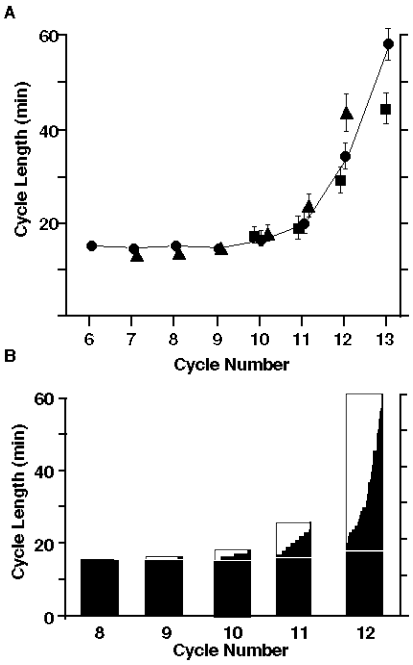

Fig. 2. Cell cycle length in individual embryos. (A) Mean cell cycle length for each cell cycle. Symbols (solid circles, triangles, squares) indicate three different embryos. Error bars indicate 70% nonparametric confidence limits calculated from the Sign Test (Fisher, 1925; Thompson, 1936). (B) Cell cycle length distributions at each cell cycle in one individual embryo. Within each column, the steps correspond to the cycle length of individual cells or small groups of cells. Horizontal lines at each cycle number indicate the longest (top line) and shortest (white line) cell cycle. Note that the distributions are not normal but uniform. (In this representation, a normal distribution, or bell-shaped curve, would be indicated by a sigmodial curve of cycle lengths at each cycle number.) Therefore, all statistical comparisons of cycle lengths between cycle numbers, and embryos as well, were based on nonparametric approximations.

basis at cycle 11 (P<0.05, Wilcoxon Rank Sum Test), and the cycles continue to lengthen progressively so by cycle 13 the average cycle length has increased more than threefold.

Throughout this time, from cycle 2 until the start of epiboly, the length of mitosis itself remains constant at 6 to 7 minutes (data not shown); hence cycle lengthening is due to lengthening of the period of interphase. Our methods do not further subdivide the interphase period.

The cycles also lose synchrony (Fig. 2B). At first, not all of cells begin to lengthen their cycles simultaneously and lengthening if it occurs at all, varies in extent. Whereas many embryos show some loss of synchrony at cycle 9, cycle 10 is the first to exhibit lengthening in most of the cells. Hence the onset of loss of synchrony approximately coincides with the onset of cycle lengthening itself. By cycle 12, the range in cycle lengths becomes dramatic; the longest are more than twice the shortest, the latter still not having changed much at all.

The loss of synchrony that we describe is not due to development of metasynchronous waves of divisions, as has been suggested for *Xenopus* (see Yasuda and Schubiger, 1992) and indirectly for zebrafish (Marrable, 1965). Many embryos do show global metasynchrony, occurring well before cycle 10 (data not shown). However, metasynchrony is invisible in the small blastoderm volume that we examined in this study. As we document below, cells with different cycle lengths are mixed together, not at all distributed in the orderly fashion that metasynchrony would predict.

Table 1. Median cell cycle lengths during zebrafish midblastula stages at 28°C

Cycle number	Median cycle length (min)	90% confidence limits* (min)
7	14.2	12.9-15.0 (*n*=9**)
8	14.5	13.8-15.5 (*n*=13)
9	15.0	14.5-15.9 (*n*=16)
10	17.0	16.1-18.0 (*n*=17)
11	22.5	20.5-27.8 (*n*=17)
12	33.5	31.6-36.7 (*n*=7)

*Nonparametric confidence limits calculated from the Sign Test (Fisher, 1925; Thompson, 1936).
**Number of embryos analysed for each cycle number.

Transcription and cell motility are activated as the cell cycle lengthens

In frogs cycle lengthening at MBT may be accompanied by other new characteristics, including activation of transcription and motility (Newport and Kirschner, 1982a). We found both changes in zebrafish as well.

To measure RNA synthesis, we injected the yolk with labeled UTP during cleavage and, at later stages, measured incorporation of label in total nucleic acids (Fig. 3). We first detected incorporation above background 3 hours after fertilization, corresponding approximately to the beginning of cycle 10. Therefore, within the sensitivity of the method (see Forbes et al., 1983; Nakakura et al., 1987), transcription is activated coincidentally with the lengthening of the cell cycle at cycle 10, and it increases progressively on per cell basis for several cycles thereafter (inset, Fig. 3).

We could directly observe pseudopod formation, a measure of motility, from our video time-lapse recordings, particularly in the case of cells labeled with lineage tracer dye (Fig. 4). Pseudopods form during interphase in rare cycle 11 cells that had particularly long interphases (>18 minutes) and, more typically, during interphase 12. Thus motility appears, on the average, one to two cycles after the beginning of cell cycle lengthening.

We observed no pseudopods at all during mitosis. Mitosing cells are spherical (Fig. 4D, after ‘m’) and appear to be high in tension, as judged by their indentation into adjacent interphase cells. Pseudopod formation is rare during a 3 minute period before nuclear membrane disappearance, when one might observe a small, quickly retracted bleb (Fig. 4E, at −1 minute and Fig. 4G, at −2 minutes).

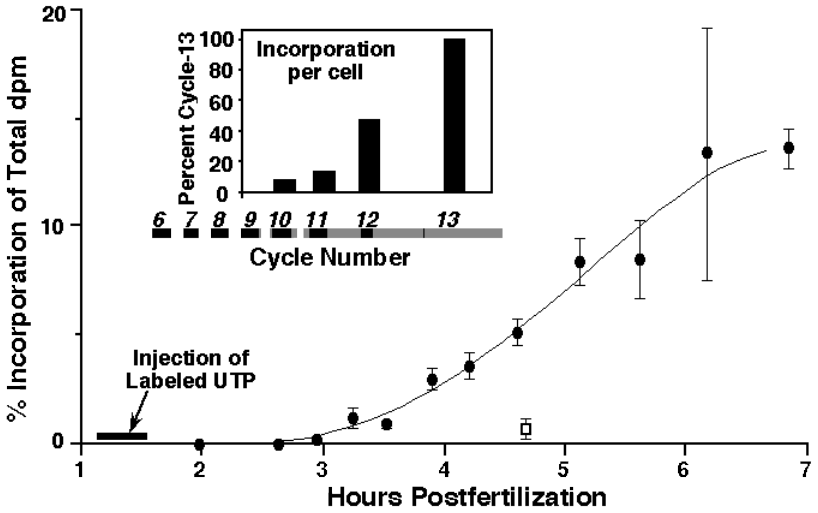

Fig. 3. Accumulation of newly synthesized RNA, showing total accumulation after injection of labeled UTP before the 8-cell stage. Each measurement (closed circles) is the ratio of counts in nuclei acids to total counts injected. Open square, RNaseA controls. Means and s.e.s are calculated from 8 combined replicate experiments (5 to 8 measurements for each point). Total number of counts per embryo was 20,000 to 100,000 disints/minute. Inset shows cellular accumulation of newly synthesized RNA, showing the median of three experiments. Bars indicate per cent incorporation of cycle 13, based on densitometry over the early appearing bands between 75 and 150 base pairs. No correction was taken for background, which was approximately half the level at cycle 10. Italicized numbers indicate cycle numbers.

Pseudopods are absent as well during early interphase: we recorded an early movement 4 minutes after cytokinesis (Fig. 4F), but the quiet period was typically several minutes longer. Collectively, our observations suggest that cells can form pseudopods only during interphases that have reached a critical length.

Onset of cycle lengthening is correlated with the nucleocytoplasmic ratio, and not with cell division number

If the nucleocytoplasmic ratio controls the onset of the MBT in zebrafish, then the cycle when both cycle lengthening and loss of synchrony occur should change in tetraploid and haploid embryos, for the nucleocytoplasmic ratios are respectively doubled and halved. As predicted, we observed that tetraploid embryos begin cell cycle lengthening about a cycle early, at cycles 8 and 9, and haploid embryos begin cell cycle lengthening about a cycle late, at cycle 11 (Fig. 5A). As in diploids, the lost of cell synchrony when ploidy is either increased or lowered coincides with the onset of cycle lengthening. This is revealed by comparison of cell cycle dispersions (Fig. 5B), which, as we have seen (Fig. 2B), is the basis for the loss of cell synchrony and a sensitive measure of it. We also observed that, in haploid embryos, cell motility begins 2 cycles later than the onset of cycle lengthening (n=3, data not shown), compared with diploids.

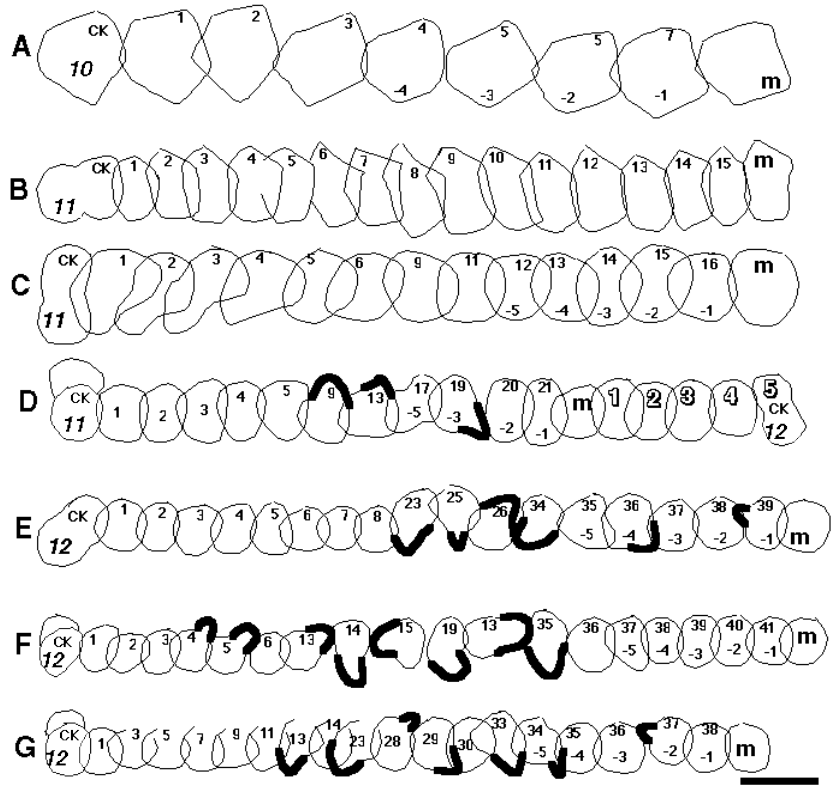

Fig. 4. Tracings of individual nonmotile and motile fluorescently labeled cells in vivo drawn from the video monitor. Thickening in the cell outlines indicate retracting or extending pseudopods. Sequences from time-lapse records were selected from cytokinesis to prophase, except for D, which extends from cytokinesis to cytokinesis, to demonstrate the rounding of the cell during mitosis. In the central portion of interphase during the time of pseudopod formation, cell outlines without active pseudopods are excluded. The italicized number in the first outline of each sequence indicates the cycle number of that cell; the number on each outline indicates the time in minutes since the beginning of interphase; the minus numbers indicate the time until the beginning of the next mitosis; outlined numbers after 'm' in D indicate minutes after the beginning of mitosis. Abbreviations: CK, cytokinesis; m, beginning of mitosis as defined by the disappearance of the nucleus. Scale bar, 40 μm.

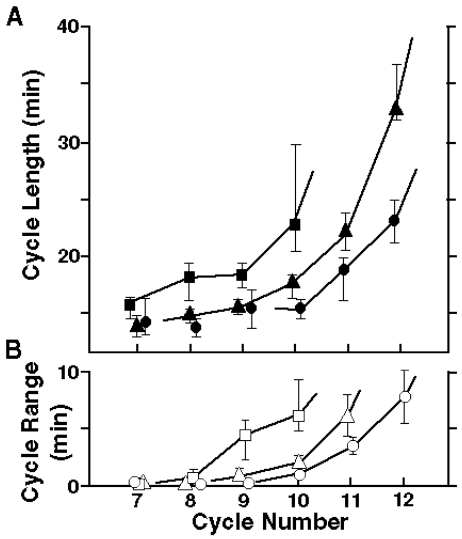

Fig. 5. Comparison of haploid (circles), diploid (triangles) and tetraploid (squares) cell cycle lengths. (A, open points) Median cell cycle lengths from cycle 7 to 12. (B, closed points) The loss of cell synchrony, measured as the median difference between the shortest and longest cell cycle lengths. Error bars indicate 70% confidence limits calculated by the Sign Test (Fisher, 1925; Thompson, 1936). Number of embryos measured: haploid, *n*=9; diploid, *n*=17; and tetraploid, *n*=4.

Hence, our observations support the model that nucleocytoplasmic ratio controls the onset of cell cycle lengthening as well as several of the behaviors associated with it.

One could make an alternative argument that the change in the tetraploid embryos could be due to a mechanism of nuclear division counting rather than control by nucleocytoplasmic ratio. This is because we create tetraploids by blocking the first cell division, but the chromosomes replicate as usual during the first cell cycle. Hence, cycle lengthening occurs after the same number of replications in diploids and tetraploids.

This argument cannot explain the cycle delay in haploids. Never-the-less, we directly tested nuclear division counting in an experiment analogous to blastomere ligature in *Xenopus* (Newport and Kirschner, 1982a) and taking advantage of cleavage in zebrafish being meroblastic, or incomplete. We removed one nucleus at the 2-cell stage to create a 'partially enucleated' embryo (Fig. 6), containing a control side and an enucleated experimental side. The control side continues to divide, but the experimental side does not divide until after a nucleus or two from the control side invades it, typically following division 6. If nuclear division counting were present, cycle lengthening would be expected to occur simultaneously in both sides of the embryo, since all of the nuclei have undergone the same number of divisions. However, the control side began cell cycle lengthening at the usual time, cycle 10 or 11, but the experimental side continued to cycle rapidly for about five additional cycles. The results are as predicted by a hypothesis for control by nucleocytoplasmic ratio, and not for a mechanism involving nuclear division counting.

A 15 minute cell cycle oscillator in water-activated eggs

The enucleation experiment just described suggests that short cell cycles can continue long beyond the ten or so that are normally present. In agreement, we observed that, if unfertilized eggs are activated by simply exposing them to water, they undergo a very long series of rapidly occurring cyclic changes characteristic of cell cycles during cleavage.

The water-activated eggs do not actually cleave, but periodically they commence cytokinesis with bizarre, unpredictably located cleavage furrows (Fig. 7A-C) that then abort. There is a nuclear cycle marked by the disappearance of the nuclear membrane during each 'mitosis' (Fig. 7D,E), and with time the nucleus becomes large and multilobed. The water-activated eggs also appear to increase in tension during mitosis and relax during interphase, allowing con-

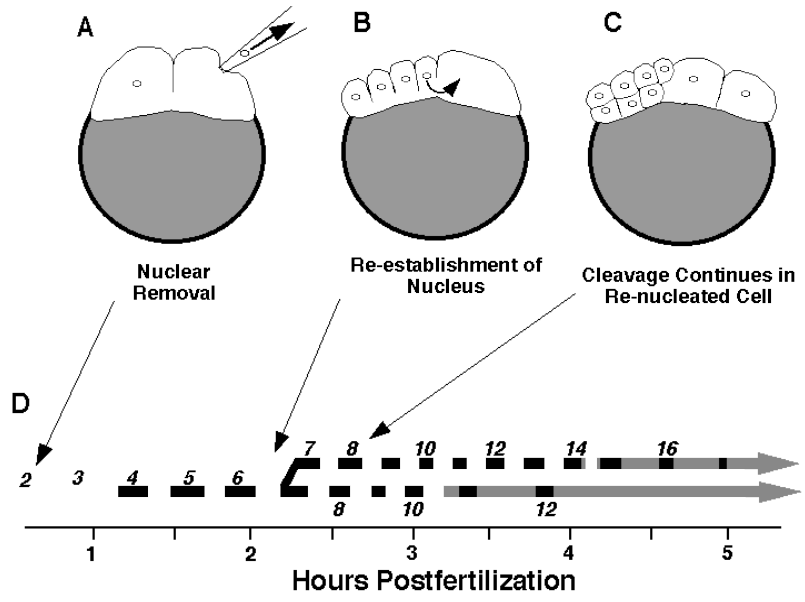

Fig. 6. Cell cycle lengthening in a partially enucleated embryo. (A-C) Schematic of experiment. (A) Nuclear removal of experimental side at the 2-cell stage. Time-lapse recording was started at cycle 4. (B) Invasion of the experimental side by nuclei from the control side, after internal cell membranes lift away from the yolk at division 6. (When this occurs varies among embryos, from cycle 5 to 7). (C) Resumption of division in the experimental side. (D) Time-lapse record of one experiment. The lower record is for the control side of the embryo and the upper record (after the bifurcation) is for the experimental side. This result is typical of five other experiments. Key to records: black portions of line indicate all cells in interphase; clear portions of line indicate all cells in mitosis; grey portions of line indicate a mixture of interphase and mitotic cells and italicized letters above record indicate cycle numbers.

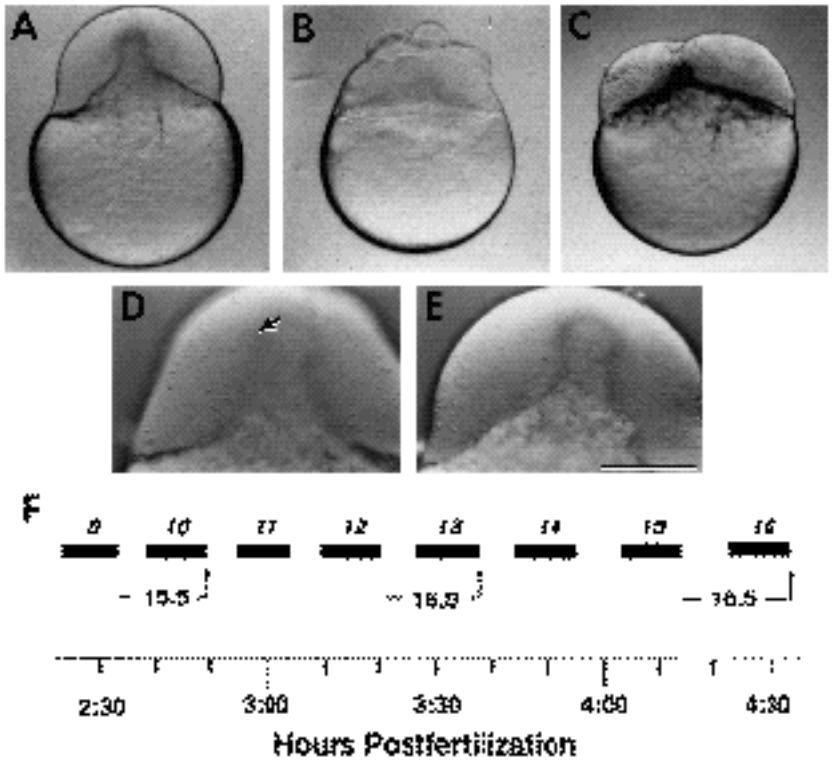

Fig. 7. Cell cycle record of activated eggs. (A) Typical water-activated egg, in 'mitosis'. (B,C) Examples of the unpredictable cleavage furrows that often appear on water-activated eggs. These furrows usually completely retract within several cell cycles. B is in 'interphase'; C is in 'mitosis'. (D,E) Higher-power view of egg in A, two cycles later. (D) Focused on the nucleus (arrow) of the egg in interphase. (E) In mitosis, 2 minutes later, the nucleus has disappeared; note the difference in cell shape compared to D. (F) Partial time-lapse record of one activated egg, which ultimately continued to cycle 21 before lysis. Arrows beneath record indicate cycle length in minutes for selected cycles. At cycle 20, the cycle length was 25 minutes in this embryo. Scale bar is 300 μm for A-C and 150 μm for D,E.

venient time-lapse recording of the cell cycle, similar in principle to the methods used to measure the surface contractions of cleavage-blocked *Xenopus* eggs (Hara et al., 1980). They never undergo the extensive cycle lengthening of normal embryos at cycle 10 through 12. For the first 15 cell cycles, the cycle period is close to that of normal cleavage, i.e. 15 minutes evenly split between mitosis and interphase (Fig. 7F). Afterwards, like a clock winding down, the period progressively slows to about 30 minutes, by the time when the eggs lyse, at about 8 hours postactivation. Thus, in water-activated eggs, cell cycle-like oscillations occur at 15 minute intervals, and do so long after the normal time of cell cycle lengthening.

Individual cell volumes and cycle lengths are correlated

We would like to understand what controls the cell cycle characteristics of individual cells, when, around cycle 10, only some of them begin cycle lengthening and do so to a variable extent. Cell position within a mitotic domain (Kane et al., 1992) appears not to play a determining role, for blastoderm cells with long and short cycles are intermixed (Fig. 8A). In contrast, in single lineages followed with the aid of dye labeling (n=21), we found that the cell cycle variation between sibs was less than between nonsibs (Fig. 8B). Furthermore, lineages that began lengthening at cycle 10 continued to contain longer than average cell cycles in subsequent cell cycles. This relationship is cell autonomous, for when dividing cells insert themselves into a distantly related family, their cycles are still comparable to one another and not necessarily to those of their new neighbors (e.g. Fig. 8A).

What differences among cycle 10 blastomeres might be transmitted in a lineage-dependent manner? One possibility is cytoplasmic volume, for at these early stages of development there is no cell growth and thus cells must inherit their volumes. We imagine an asymmetric division could generate a pair of sibs that differ in volume. In keeping with control by the nucleocytoplasmic ratio, the sibs would cycle at different rates, and generate lineages of cells cycling at different rates, a lineage of small cells cycling relatively more slowly than a lineage of large cells.

To examine this possibility, we directly determined cell volumes from cycle 10 through 13, and kept track of lineage relationships and cycle lengths within the descendent families. In control measurements, the summed volume of each daughter pair equaled that of the mother cell (s.d.=7%), showing the precision of the measurement and confirming that the cells are not growing during these stages. Asymmetric divisions were indeed present and resulted in immediate changes in the length of the subsequent cycle (Fig. 8C). These differences are inherited, so that at least two cycles later, the lineages still reflect the unequal division, with the descendants of the smaller cell always possessing the longer cell cycles. When we compare volume to cycle length (Fig. 8D), cell volume, not cycle number, is the best predictor of cycle length from cycle 10 until mid cycle 13.

Asymmetric divisions must be common, for within a single cycle there is more than a twofold difference in the volumes of the smallest and largest cells (Fig. 8D). We were unable to explore the extent of unequal division before cycle 10 because cells do not completely round up during mitosis throughout early cleavage. However, based on the distribution of cell size at seen in cycle 10, unequal cleavages are likely to be occurring earlier, as would account for observed variability in volume, and hence cycle length.

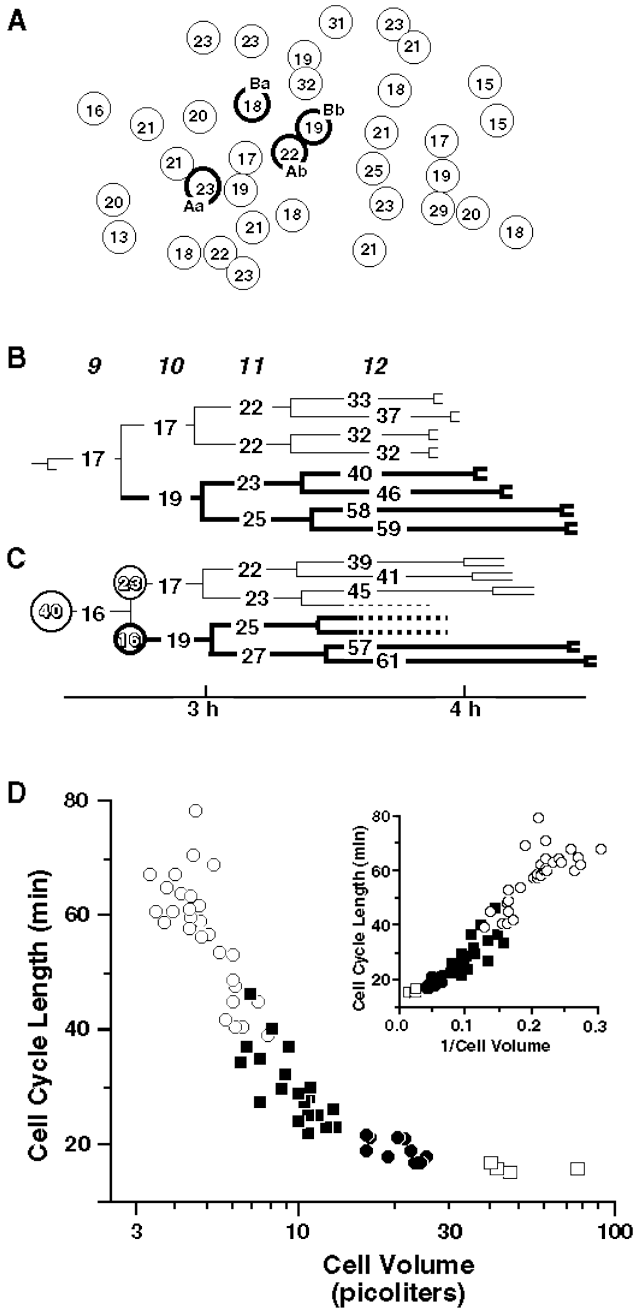

Fig. 8. Relationship between lineage, cell volume and cycle length. (A) Cells of different cycle lengths mix freely in the blastoderm, and appear independent of the cycle length of adjacent cells. View of nuclei (circles) in a 150×80×60 μm portion of the blastoderm at cycle 11, in which the cell cycle lengths (number inside of nuclei, in minutes) of all the cells were measured. The lettered cells are descended from a single cycle 9 cell. A and B are first cousins and a and b are siblings. The spreading of the clone is caused mainly by cell divisions, not interphase movements, until cycle 12. (B) Initiation of cycle lengthening predicts relative cycle length in subsequent cycles. Diagram portrays two sublineages that arose from a single cell which was labeled with lineage dye before cycle lengthening began. The sublineage which began lengthening at cycle 10 (bold lines) contained the longest cell cycle lengths in subsequent cycles compared to the sublineage that began lengthening in cycle 11 (thin lines). This is typical of 18/21 other dye-traced lineages. (C) Lineage containing an asymmetric cleavage, with respect to cell volume, at division 9. The change in cell cycle length occurs in the next cycle, cycle 10, and the effects of the unequal division continue to be seen several cycles later. Outlined numbers within circles indicate cell volume (in picoliters). Dashed lines indicate cells that drifted out of the field of view. For B,C: numbers within the lineage tree indicate the cell cycle length in minutes; italicized numbers above the lineage diagrams indicate cycle numbers; abscissa beneath lineage diagrams indicates time postfertilization. (D) Correlation of cell volume and cell cycle length. Measurements are of single deep cells during mitosis all in one individual embryo. The inset shows the same data as a double reciprocal plot. (Note: cell cycle length=1/division rate.) Open squares, cycle 10; closed circles, cycle 11; closed squares, cycle 12; open circles, cycle 13. Individual linear correlations for cycle 11, cycle 12, and early half of cycle 13 are each statistically significant (P<0.025).

DISCUSSION

Zebrafish midblastula transition begins at cycle 10

The lengthening of the cell cycle is the distinguishing event of *Drosophila* and *Xenopus* MBT (Edgar and Schubiger, 1986; Kimelman et al., 1987). In the zebrafish, this lengthening begins in some cells at cycle 10 and, by cycle 12, all of the cell cycles are long, some dramatically so. *Xenopus* MBT is marked by loss of cell synchrony and activation of both motility and transcription; likewise, in the zebrafish, these behaviors occur as the cell cycle lengthens.

In *Xenopus*, the appearance of asynchrony and motility, and activation of transcription are thought to result from the MBT cycle lengthening (Kimelman et al., 1987). Although we have not experimentally verified that this is also the case in zebrafish, the behaviors associated with cycle lengthening occur in a manner such that lengthening could be the cause in this species as well. The embryo begins to lose synchrony at cycle 10 because cycle lengthening begins in some cells before others (Fig. 2). After transcription is activated at zebrafish cycle 10, in each subsequent cycle the amount of transcription per cell roughly correlates with the increase in length of interphase at that cycle (Fig. 3). Lastly, in our studies of individual cells during cycle 11 and 12, only those cells possessing a long cell cycle are motile (Fig. 4).

The nucleocytoplasmic ratio seems to govern the initiation of MBT

Our recordings of water-activated eggs demonstrate the existence of a cell cycle oscillator, possibly similar to that found in early *Xenopus* cleavage-blocked eggs (Hara et al., 1980). This oscillator in zebrafish has a 15 minute period, the cleavage cell cycle length and is capable of continuing long past the typical time of MBT (Fig. 7).

We show further that during normal development this oscillator is pre-empted when the embryo attains a critical nucleocytoplasmic ratio (Fig. 5). The development of the partially enucleated embryo (Fig. 6) argues against other models for timing of the MBT, such as absolute time post-

fertilization or a division-counting mechanism. This is because the experimental side of the partially enucleated embryo reaches MBT at a different time and after a different number of divisions than the control side. Furthermore, this experiment argues against a global control of MBT, since MBT occurs at two different times in the same embryo.

The nucleocytoplasmic ratio may continue to regulate autonomously the cycle length of individual cells during a MBT period

We suggest that the partially enucleated embryo in fact presents an experimentally created, albeit extreme, demonstration of processes present in normal embryos at MBT. Here too, cycle lengthening begins asynchronously and our evidence suggests that, as in the experimental situation, asynchrony is due to volume differences among the cells (Fig. 8). The differences could arise because of unequal early divisions; we directly observed that they occur at midblastula cycles. Perhaps, throughout the major extent of the blastoderm (Kane et al., 1992), division asymmetry is due only to random noise in the control of cytokinesis.

With no growth during interphases, the volume differences among cells are inherited, autonomously and in a lineage-dependent fashion, and cycle lengths differ in these lineages. *When* cycle lengthening begins predicts the subsequent *degree* of lengthening in the same cell lineage.

We observed that the cycle lengths during three cell cycles following the initiation of MBT directly reflects cell volumes (Fig. 8D). To explain the cycle length dependence on volume, we extend the hypothesis for initiation of MBT. Our experiments suggest that, as has been well documented in other creatures, the *initial* cell cycle lengthening of MBT is controlled by the nucleocytoplasmic ratio. We propose that the relationship between the volume of the cytoplasm and the nucleus continues for several cycles after the beginning of MBT, so that during a MBT *'period'* the nucleocytoplasmic ratio constantly regulates the cell cycle length — the higher the nucleocytoplasmic ratio, the longer the cell cycle. Our observation that during the MBT period, cycle length varies directly with the reciprocal of cell volume supports this hypothesis.

The basis for control of the initiation of MBT by the nucleocytoplasmic ratio is hypothesized to be a titration of a maternally supplied cytoplasmic component that is necessary for maintenance of the cell cycle (Newport and Kirschner, 1982b). Thus, the end of the MBT period might be formally defined as the time when this titration is complete, and nucleocytoplasmic ratio no longer controls cycle length. At such a point, the cell cycle may either arrest or be controlled zygotically. At least in *Drosophila* this stage is reached during cycle 14 when the zygotic gene *string* is necessary for initiation of the cell cycle (Edgar and O'Farrell, 1989) and gene activity is necessary for the formation of at least some of the cycle 14 mitotic domains (Arora and Nüsslein-Volhard, 1992). Mitotic domains also form during the MBT period in zebrafish (Kane et al., 1992) and the perturbation of these domains in α-amanitin-treated embryos (Kane, unpublished observations) argues that the end of the MBT period is in late cycle 13, approximately 2 hours following the initiation of MBT. Mutational analysis in zebrafish, now underway (Strähle and Ingham, 1992), may help elucidate the nature of zygotic gene control of this interesting period of development.

We would like to thank John Postlethwait, Vicki Chandler, Tadmiri Venkatesh and James Weston, as well as all the members of the University of Oregon zebrafish group, for their critical comments on early versions of this manuscript, and their patience. We thank Charline Walker for production of haploid and tetraploid embryos, Reida Kimmel for assistance with photography and Paul Myers for assistance with computer interfacing, and Rachel Warga for her kind encouragement. This work was supported by NIH Grant 5 T32 GM07413 10 and NSF Grant BNS 9009544.

REFERENCES

Arora, K. and Nüsslein-Volhard, C. (1992). Altered mitotic domains reveal fate map changes in Drosophila embryos mutant for zygotic dorsoventral patterning genes. *Development* **114**, 1003-1027.

Bissen, S. T. and Weisblat, D. A. (1989). The durations and compositions of cell cycles in embryos of the leech, *Helobdella triserialis. Development* **106**, 105-118.

Edgar, B. A. and O'Farrell, P. H. (1989). Genetic control of cell division patterns in the Drosophila embryo. *Cell* **57**, 177-187.

Edgar, B. A. and Schubiger, G. (1986). Parameters controlling transcriptional activation during early Drosophila development. *Cell* **44**, 871-877.

Fisher, R. A. (1925). *Statistical Methods of Research Workers.* Edinburgh: Oliver and Boyd.

Foe, V. E. (1989). Mitotic domains reveal early commitment of cells in *Drosophila* embryos. *Development* **107**, 1-22.

Forbes, D. J., Kornberg, T. B. and Kirschner, M. W. (1983). Small nuclear RNA transcription and ribonucleoprotein assembly in early Xenopus development. *J. Cell Biol.* **97**, 62-72.

Gerhart, J. C. (1980). Mechanisms regulating pattern formation in the amphibian egg and early embryo. In *Biological Regulation and Development* (ed. R. F. Goldberg), 133-150. New York: Plenum Press.

Hara, K., Tydeman, P. and Kirschner, M. (1980). A cytoplasmic clock with the same period as the division cycle in Xenopus. *Proc. Natl. Acad. Sci. USA* **77**, 462-466.

Hisaoka, K. K. and Battle, H. I. (1958). The normal development stages of the zebrafish, *Brachydanio rerio* (Hamilton-Buchanan). *J. Morphol.* **102**, 311-328.

Ho, R. K. and Kane, D. A. (1990). Cell-autonomous action of zebrafish spt-1 mutation in specific mesodermal precursors. *Nature* **348**, 728-30.

Kane, D. A. and Warga, R. M. (1991). Zebrafish development. In *A Dozen Eggs: Time-lapse Microscopy of Normal Development* (ed. R. Fink), Segment 9. Sunderland: Sinauer

Kane, D. A., Warga, R. M. and Kimmel, C. B. (1992). Mitotic domains in the early embryo of the zebrafish. *Nature* **360**, 735-737.

Kimelman, D., Kirschner, M. and Scherson, T. (1987). The events of the midblastula transition in Xenopus are regulated by changes in the cell cycle. *Cell* **48**, 399-407.

Kimmel, C. B., Warga, R. M. and Schilling, T. F. (1990). Origin and organization of the zebrafish fate map. *Development* **108**, 581-94.

Kobayakawa, Y. and Kubota, H. (1981). Temporal pattern of cleavage and the onset of gastrulation in amphibian embryos developed from eggs with reduced cytoplasm. *J. Embryol. Exp. Morphol.* **62**, 83-94.

Maniatis, T., Fritsch, E. F. and Sambrook, J. (1982). *Molecular Cloning.* Cold Spring Harbor, New York: Cold Spring Harbor Laboratory.

Marrable, A. W. (1959). Variations in early cleavage of the zebrafish. *Nature* **184**, 1160-1161.

Marrable, A. W. (1965). Cell numbers during cleavage of the zebrafish egg. *J. Embryol. Exp. Morph.* **14**, 15-24.

Mita, I. and Obata, C. (1984). Timing of morphogenetic events in tetraploid starfish embryos. *J. Exp. Zool.* **229**, 215-222.

Myers, P. Z. and Bastiani, M. J. (1991). Neurovideo: a program for capturing and processing time-lapse video. *Computer Methods and Programs in Biomedicine* **34**, 27-33.

Nakakura, N., Miura, T., Yamana, K., Ito, A. and Shiokawa, K. (1987). Synthesis of heterogeneous mRNA-like RNA and low-molecular-weight

RNA before the midblastula transition in embryos of Xenopus laevis. *Dev. Biol.* **123**, 421-429.

Newport, J. and Kirschner, M. (1982a). A major developmental transition in early Xenopus embryos: I. Characterization and timing of cellular changes at the midblastula stage. *Cell* **30**, 675-686.

Newport, J. and Kirschner, M. (1982b). A major developmental transition in early Xenopus embryos: II. Control of the onset of transcription. *Cell* **30**, 687-696.

Okazaki, K. (1975). Normal development to metamorphosis. In *The Sea Urchin Embryo: Biochemistry and Morphogenesis* (ed. G. Czihak), 177-200. Berlin and New York: Springer-Verlag.

Oppenheimer, J. M. (1936). The development of isolated blastoderms of Fundulus heterclitus. *J. Exp. Zool.* **72**, 247-279.

Oppenheimer, J. M. (1937). The normal stages of *Fundulus heteroclitus*. *Anat. Rec.* **68**, 1-15.

Roosen-Runge, E. (1938). On the early development—bipolar differentiation and cleavage—of the zebra fish, *Brachydanio rerio*. *Biol. Bull. Mar. Biol. Lab. Woods Hole* **75**, 119-133.

Rott, N. N. and Sheveleva, G. A. (1967). Changes in the rate of cell divisions in the course of early development of diploid and haploid loach embryos. *J. Embryol. Exp. Morph.* **20**, 141-150.

Signoret, J., and Lefresne, J. (1973). Contribution a l'etude de la segmentation de l'oeuf d'Axolotl. II. Influence de modifications du noyau et de cytoplasme sur les modalités de la segmentation. *Ann. Embryol. Morphol.* **6**, 200-307.

Signoret, J. and Lefresne, J. (1971). Contribution a L'etude de la segmentation de l'oeuf d'axolotl: I. Definition de la transition blastuleenne. *Ann. Embryol. Morphog.* **4**, 113.

Spemann, H. (1938). *Embryonic Development and Induction.* New Haven: Yale University Press.

Strähle, U. and Ingham, P. W. (1992). Flight of fancy or a major new school? *Current Biology* **2**, 135-139.

Streisinger, G., Walker, C., Dower, N., Knauber, D. and Singer, F. (1981). Production of clones of homozygous diploid zebrafish, *Branchydanio rerio. Nature* **291**, 293-296.

Sulston, J. E., Schierenberg, E., White, J. G. and Thomson, J. N. (1983). The embryonic lineage of the nemotode Caenorhabditis elegans. *Dev. Biol.* **100**, 64-119.

Thomas, R. G. and Waterman, R. E. (1978). *Gastrulation in the Teleost*. Chicago: IIT Research Inst.

Thompson, M. L. (1936). On confidence ranges for the median and other expectation distributions for populations of unknown distribution form. *Ann. Math. Statist.* **7**, 122-128.

Trinkaus, J. P. and Erickson, C. A. (1983). Locomotion of Fundulus deep cells during gastrulation. *Amer. Zool.* **21**, 401-411.

Warga, R. M. and Kimmel, C. B. (1990). Cell movements during epiboly and gastrulation in zebrafish. *Development* **108**, 569-80.

Yasuda, G. K. and Schubiger, G. (1992). Temporal regulation on the early embryo: is MBT too good to be true? *Trends in Genetics* **8**, 124-127.

(Accepted 28 May 1993)